

Keywords: cycling loads; sensor; instrumented pedal; 3-component load cell; pedal patterns; global regression method; strain gauge based

Sien DIELTIENS*, Jordi D'HONDT, Marc JUWET

KU Leuven

Gebroeders de Smetstraat 1, 9000 Gent, Belgium

Mark VERSTHEYHE

KU Leuven

Spoorwegstraat 12, 8200 Brugge, Belgium

*Corresponding author. E-mail: sien.dieltiens@kuleuven.be

DEVELOPMENT OF A LOW-COST MEASUREMENT SYSTEM TO DETERMINE 3-DIMENSIONAL PEDAL LOADS DURING IN-SITU CYCLING

Summary. As increasingly more bicycles are equipped with electrically powered pedal assistance, they can become the solution for the continuous congestion that threatens Europe. Pedal assistance decreases the effort, though cyclists often experience sores that occur at the low back, knees and bottom area. The risk of injuries is predominantly determined by the pedal technique, which is highly dependent of bicycle design, seat type and cycling posture. The optimal cycling technique and the relation to the bicycle characteristics needs to be discovered to create guidelines for bicycle construction and usage. This paper presents the design of a low-cost measurement system to analyse three-dimensional pedal loads in function of the pedal cycle by an instrumented pedal and an absolute encoder fixated on the crank. The pedal proposed is a combination of a unique steel sensor with twelve sensor regions, organized in four full Wheatstone bridges, installed on a standard pedal spindle. The pedals are calibrated with the Global Regression method acquiring a calibration matrix with a standard error percentage of full scale of maximum 0.5%. The instrumented pedal distinguishes itself from state-of-the-art techniques through (i) compatibility: it fits on every conventional bicycle, (ii) compactness: not influencing the cycling kinematics, (iii) broad applicability: it is applicable for in-situ measurements with extreme manoeuvres and (iv) accuracy: it delivers a relative high accuracy in relation to the production precision and production costs.

1. INTRODUCTION

Continuous congestion threatens the European logistics performance and overall economy. Traditional bicycles form a good solution in cities; they do not emit exhaust gases, take up less space, are less noisy and encourage people to exercise, though are too slow and strenuous for longer intercity rides. The introduction of electrically powered pedal assistance on city bikes has changed the situation drastically. Pedal assistance reduces cycling effort, increasing the cycling population and the cycling distances. Implementing pedal assistance on cargo bikes makes them more attractive for freight transport, reducing the usage of heavy goods vehicles in city centers.

Unlike the bicycle racing industry, there is no research dedicated to user-induced cycling forces acting on bicycles with pedal assistance. Nevertheless, it is of interest for a lot more people, and the risk of overuse injuries is augmented owing to the enlarged cycling distance [1]. As injuries most often occur at the low back, knees and bottom area [2], the influence of pedal technique is crucial. Based on

pedal load patterns, joint burden and muscle fatigue can be derived and an ideal situation can be determined. Knowledge of the ideal pedal load patterns is needed to maximize cycling comfort and reduce the usage of cars and other heavy goods vehicles.

Various load cells are developed to measure pedal load patterns distinguishable by measurement location and method, as most essential ones are (i) strain gauge-based pedals, (ii) piezoelectric based pedals and (iii) strain gauge-based crank arms. This study presents a design based on strain gauge-based pedals. The instrumented pedals contain deformable structural elements equipped with strain gauges. Through a calibration procedure, forces can be related to the measured stress in the material. Hull and Davis [3] were the first to create strain gauge-based instrumented pedals that measured all three orthogonal forces and moments simultaneously to the position of the pedal along the pedal arc. The design was cumbersome and therefore only applicable on stationary bicycles in the laboratory environment. In the past decades, several new pedal sensors were developed, though they share a number of shortcomings: (i) they measure only the normal and anterior forces, ignoring the lateral ones that are accountable for severe knee injuries [3 - 6]; (ii) they are too bulky and therefore limited to the laboratory environment which is not representative for in-situ cycling [3, 4, 7]; and (iii) they lift the foot too far above the pedal spindle which influences the cyclist's pedal technique [7]. For the racing industry, multiple compact instrumented pedals are placed on the market that measure power output [8]. Again, only two-directional forces are recorded, and it is impossible to analyze the raw data. This paper presents the construction method and validation of an accurate instrumented pedal with similar dimensions as a standard pedal that measures the pedal loading in all three dimensions. The development of the improved instrumented pedal is essential to analyze the influence of differences in pedal assistance, bicycle geometry or weight distribution (e.g. cargo bikes), shapes of seats, cycling postures, cycling duration, etc. on cycling comfort.

2. MATERIALS AND METHODS

The instrumented pedal should comply with the following requirements:

- The pedal can be mounted on conventional bicycles.
- The vertical distance between footplate and spindle is between 10 and 20 mm to adapt a normal pedal movement [7].
- The vertical distance between the underside of the pedal and spindle is at least 20 mm to prevent hitting the ground when turning.
- The system is applicable for in-situ cycling and stationary cycling.
- Anterior-posterior, medial-lateral and proximal-distal forces are measured, as they are important for overuse injuries and muscle fatigue [9].
- The full scale standard deviation is maximal of 2%. A higher accuracy is only essential to determine absolute values, not to compare the progress of mean force patterns.
- The resolution of the loads is 1 N.
- The fundamental frequency is minimal of 35 Hz [3].
- The reference frame is fixed in space.

2.1. Sensor

A patented low-cost instrumented pedal is produced that fulfills the aforementioned requirement. A unique 3-component load cell is combined with a standard bicycle spindle and a protective casing. The shape of the load cell is determined by a stress simulation with finite element analysis under the maximal pedaling loading of a competitive cyclist to prevent plastic deformations and maximize elastic deformations (Table 1). The sensor is constructed from a single block of steel, avoiding slippage of fasteners, reducing the hysteresis effect.

Table 1

Maximal pedal loads applied by a competitive cyclist

Load	Direction	Abbreviation
300 N	Anterior-posterior	X
200 N	Medial-Lateral	Y
1000 N	Proximal-distal	Z

The order of magnitude of the forces varies in function of the direction: medial-lateral (Y) forces are the smallest (200 N), followed by the slightly larger anterior-posterior (X) forces (300 N) and the five times larger proximal-distal (Z) forces (1000 N). The sensor is shaped to make deformations considerably proportional in every direction by weakening the Y sides and strengthening the Z sides. Standard pedal bearings are implemented to guarantee a long lifespan (Fig. 1a). It is compatible with the spindle of a standard bicycle to avoid turning the unconventional left thread of the left pedal spindle (Fig. 1b).

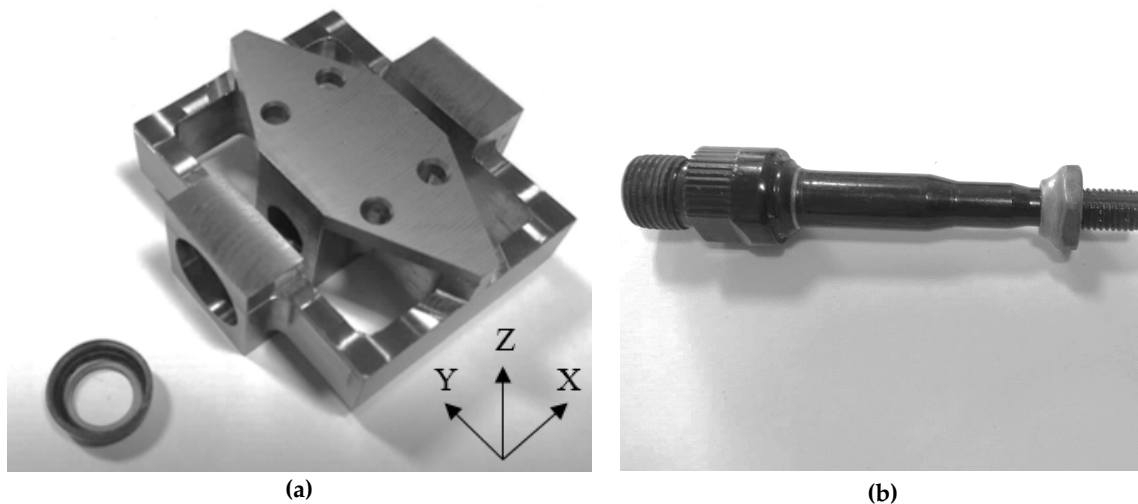


Fig. 1. Unique sensor with standard bearing (a). Standard pedal spindle (b)

The pedal contains twelve sensor regions, four in each dimension, which elastically deform during cycling (Figure 2). Strain gauges are attached in the deflection regions causing change of inner resistance during deformation. The medial-lateral, proximal-distal and vertical forces are essentially measured by four strain gauges attached in respectively the sagittal, frontal plane and transversal plane. The strain gauges are connected diagonally to avoid the influence of a traversing central of application caused by foot movement. The output signals are arranged in a Full Wheatstone Bridge for amplification and to diminish the effect of external factors such as humidity and temperature.

2.2. Pedal Angle

The current pedaling load coordinate system is local and has no fixed attitude in the bicycle coordinate reference frame. The orientation of the pedal is recorded in relation to the ground surface to determine the X', Y' and Z' forces in the global reference frame. The InvenSense MPU-6050 sensor is attached on the bottom side of the center of the pedal to measure pedal angle. The chip contains a MEMS accelerometer and MEMS gyroscope. It accommodates separate 16-bits ADC hardware for the three dimensions.

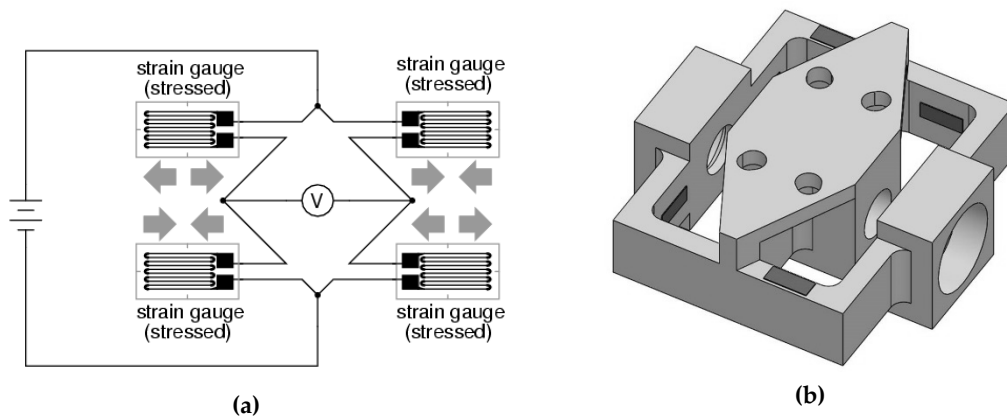


Fig. 2. Full bridge configuration of strain gauges (a). Application on the sensor (b)

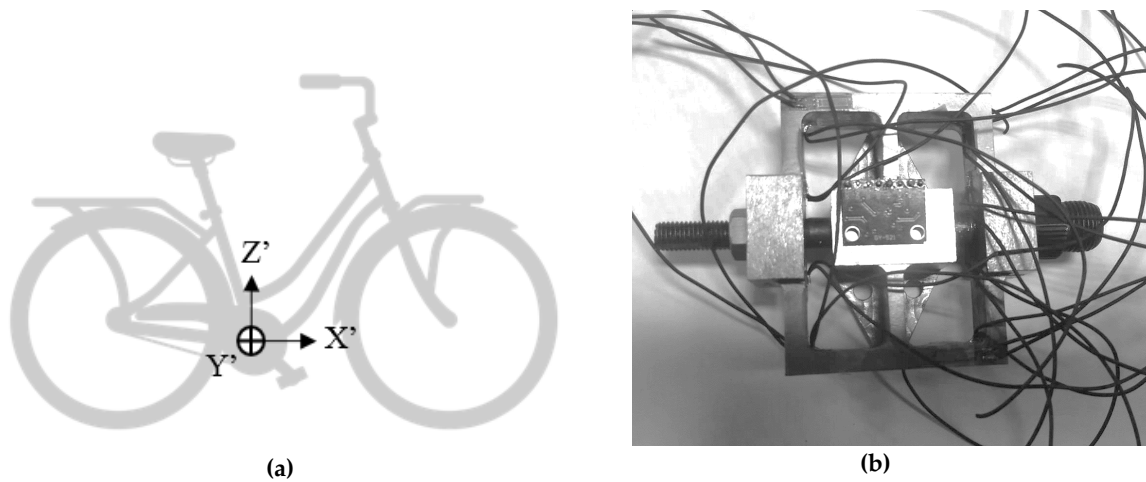


Fig. 3. Global reference frame (a). MPU-6050 sensor attached on bottom side of sensor (b)

2.3. Calibration

The output signals of the three full-bridge strain gauge configurations are expressed in mV/V. The related cycling loads, expressed in N, are derived by the Least Square Global Regression Method: a calibration matrix is set up to capture the relation between multidirectional forces and the output signals of all three full-bridge strain gauge configurations [10]. The pedaling frequency is below 5 Hz, which makes dynamical calibration superfluous [11].

Hundred measurements are taken in which the pedal is orientated at various angles in the sagittal and frontal planes, and different weights are attached. The weights are measured utilizing a balance with a precision of 0.1 gram. The MPU-6050 sensor measures the orientation of the pedal with a precision of 0.1° , and isolated forces are calculated in the X', Y' and Z' directions. The maximally applied isolated forces are analogue to the peak pedal forces of a conventional cyclist described by Mornieux et al: 180 N in the X direction, 100 N in the Y direction and 500 N in the Z direction [12] (Table 2). Within this region, the sensor's behavior is linear. The hysteresis effect is taken into account by changing the sequencing of the loads and comparing the results.

Table 2

Maximal pedal loads applied by a recreational cyclist

Range	Direction	Abbreviation
0 - 180N	Anterior-posterior	X
0 - 100N	Medial-Lateral	Y
0 - 500N	Proximal-distal	Z

Strain gauges essentially measure longitudinal strain: the full-bridge strain gauge configuration in the frontal plane principally measures X forces, the configuration in the sagittal plane measures Y forces and the configuration in the transversal plane measures Z forces. Under multidirectional loading, strain gauges react additionally on transversal forces due to their inner cross-sensitivity and construction imperfections of the sensor like minor misalignments. A calibration matrix exposes the relation between all three full-bridge strain gauge configurations (m_{FX} , m_{FY} and m_{FZ}) and multidirectional pedal loading (F_X , F_Y and F_Z), given by (1).

$$\begin{bmatrix} C_{11} & C_{12} & C_{13} \\ C_{21} & C_{22} & C_{23} \\ C_{31} & C_{32} & C_{33} \end{bmatrix} \begin{bmatrix} m_{FX} \\ m_{FY} \\ m_{FZ} \end{bmatrix} = \begin{bmatrix} F_X \\ F_Y \\ F_Z \end{bmatrix} \quad (1)$$

The calibration matrix is derived from the following formula (2):

$$\begin{bmatrix} C_{11} & C_{12} & C_{13} \\ C_{21} & C_{22} & C_{23} \\ C_{31} & C_{32} & C_{33} \end{bmatrix} = \quad (2)$$

$$\left(\begin{bmatrix} m_{FX1} & m_{FX100} \\ m_{FY1} & \dots & m_{FY100} \\ m_{FZ1} & m_{FZ100} \end{bmatrix} \begin{bmatrix} m_{FX1} & m_{FX100} \\ m_{FY1} & \dots & m_{FY100} \\ m_{FZ1} & m_{FZ100} \end{bmatrix}^T \right)^{-1} \begin{bmatrix} m_{FX1} & m_{FX100} \\ m_{FY1} & \dots & m_{FY100} \\ m_{FZ1} & m_{FZ100} \end{bmatrix}^T \begin{bmatrix} F_{X1} & F_{X100} \\ F_{Y1} & \dots & F_{Y100} \\ F_{Z1} & F_{Z100} \end{bmatrix}$$

The accuracy is described by the maximal error percentage of full scale (max. error % FS), given by (3) and the standard error percentage of full scale (std. error % FS) given by (4) to efficiently compare our method with other studies [13]. The maximal error describes the maximal error found between the calculated and measured values, whereas the standard error quantifies the amount of variation.

$$\text{max. error \% FS} = \frac{\text{Max} |m_{F_i} - F_i|}{FS} 100 \quad (3)$$

$$\text{std. error \% FS} = \sqrt{\frac{\sum_{i=1}^N (m_{F_i} - F_i)^2 / (N-f)}{FS}} 100 \quad (4)$$

where N = number of samples and f = degrees of freedom of the calibration matrix

2.4. Pedal cycle

To properly analyze the pedaling motion of a human subject, the cycling loads are expressed in function of one pedal cycle. An absolute encoder is developed to measure the position of the pedal arm (Fig. 4b). The encoder is constructed from a toothed metal disk fixated on the pedal arm and an optical sensor fixated on the frame. The sensor counts the gaps, starting from a wider reference gap, providing an absolute reference angle. Combining information from the encoder and the instrumented pedal, average pedal cycles are constructed and compared for analysis.

2.5. Data acquisition

Data acquisition is provided by combining National Instruments' cDAQ-9178 chassis with the universal analogue input module NI9219 for the strain gauges and the universal analogue input module NI9215 for the encoder. The data acquisition system automatically synchronizes the data from the different ports, adds a time stamp and transfers it to a notebook by cable. The data are recorded and analyzed with Matlab. A third order butterworth low-pass filter is applied, and mean pedal cycles are determined.



Fig. 4. Unique incremental encoder combining a toothed metal disk and an optical sensor

3. RESULTS

The following table addresses the calculated accuracy of the calibration matrix (Table 3).

Calibration matrix Accuracy

Table 3

Direction	Max. error % FS	Std. error % FS
X	3.0854	0.5386
Y	3.6366	0.3280
Z	1.6555	0.1514

The maximal error percentage of full scale is the largest in the medial-lateral direction (3.6366%), followed by the anterior-posterior direction (3.0854%) and the proximal-distal direction (1.6555%). The standard error percentage of full scale is the largest in the anterior-posterior direction (0.5386%), followed by the medial-lateral direction (0.3280%) and the proximal-distal direction (0.1514%).

The following graphs present a typical cycling pattern of a recreational cyclist of 77 kg on a woman's city bike during 15 minutes of relaxed cycling next to a canal, without turns, at a constant speed of 12 km/h on smooth pavement. The mean power of both legs is 170 W and pedaling speed is 50 rpm. The seat to pedal distance is set as 92 percent of the inner leg length. The curves present the mean proximal-distal, anterior-posterior and medial-lateral directional forces [N] expressed in function of one pedal cycle [%] where the right pedal starts (0%) and ends (100%) in the upper dead center. The gray area represents two times the standard deviation (95% of all measurements).

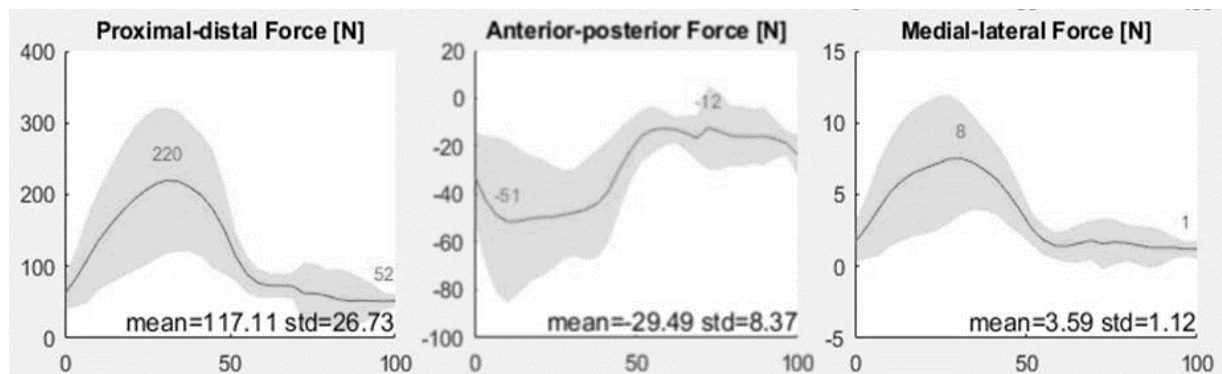


Fig. 5. The mean proximal-distal, anterior-posterior and medial-lateral directional forces [N] are expressed in function of one pedal cycle [%]

The Z force is directed distally during the whole pedal cycle. It is limited when the pedal is in the region of his upper and lower dead center. At 348 degrees, it reaches a minimum of 52 N. After the dead center, it smoothly increases until its maximal value of 220 N at 120 degrees. In this phase, most power is built up (power phase). When the first half of the pedal cycle is completed, the left pedal takes over and a limited force is transmitted over the right pedal (recovery phase). The X force is directed anteriorly during the whole pedal cycle. Similar to the Z force most power is built up in the power phase and least in the recovery. The maximal value is 51 N at 48 degrees and the minimal value is 12 N at 264 degrees. The maximal X force occurs in the first half of the power phase, whereas the maximal Z force occurs 72 degrees later in the second half of the power phase. The minimal X value manifests itself in the first half of the recovery phase whereas the minimal Z value manifests itself 102 degrees later in the second half of the recovery phase. In addition, the Y forces are directed laterally. The location of the peak values is similar to the Z force. A maximum of 8N is found in the second half of the power phase at 120 degrees and a minimum of 1 N is found in the second half of the recovery phase at 348 degrees.

4. DISCUSSION

The accuracy of the calibration matrix is not often described in pedal sensor research, and the methodology is not standardized. Newmiller et al present a maximal error of full scale of the same region (2.8%), though do not mention the standard deviation or standard error [4]. Mornieux et al described a standard error of -3.06% for the vertical dimension, -3.37% for the horizontal dimension and -2.81% for the lateral dimension [12]. The standard error percentage of full scale acquired in this research is factor 10 times smaller; therefore, the accuracy of the static calibration is satisfactory. A higher accuracy can be obtained by calibration with specific calibration equipment like a three-dimensional tensile tester. Sensors calibrated with this machinery can lead to a standard error less than 0.1% [13 - 15], though are really expensive. Furthermore, an increased amount of samples enlarges the calibration accuracy. The results acquired in this study are in agreement with previous studies [16], [17, 3, 18, 12]. The following figure presents a comparison of the outcomes of this research with that of Mornieux et al. [12].

The unidirectional patterns are considerably similar. Most power is built up in the power phase and least in the recovery. The maximal vertical and medial-lateral force is found in the second half of the power phase which matches the results of this research. The maximal anterior-posterior force is found at 90° , which differs from the results of this research (48°) caused by an extra local drop in the graph due to user-independent pedal technique, though the main inflection point is similar. The amplitude ratios match the results of this research; nevertheless, the amplitude is extremely enlarged owing to the intensity of cycling. Mornieux tested at a higher power output (300 W versus 170 W) and higher rpm (90 rpm instead of 50 rpm). The direction of anterior-posterior forces differs owing to inter-individual variations in ankle angle. The test subject of this research adopted a continue dorsiflexion, which leads to only negative X-values.

The instrumented pedal will be utilized for further research addressing bicycle design, posture, pedal technique, muscle fatigue or joint burden [1, 2, 9] to optimize cycling comfort. Here for the loading patterns need to be interpreted. The continuous dorsiflexion of the test subject leads to a reduced mechanical efficiency and an inefficient muscle activity of the gastrocnemius lateralis [19]. Lateral foot loading increases the medial contact loading of the knee joint, whereas the medial foot loading reduces it. For patients with medial gonarthrotic, it is fundamental to correct this pedal technique and minimize the lateral loading [20]. The next step is to link the different cycling techniques to the bicycle design, amount of pedal assistance, seat type, cycling posture, user's body characteristics and find an optimum to optimize cycling comfort and encourage more people to cycle.

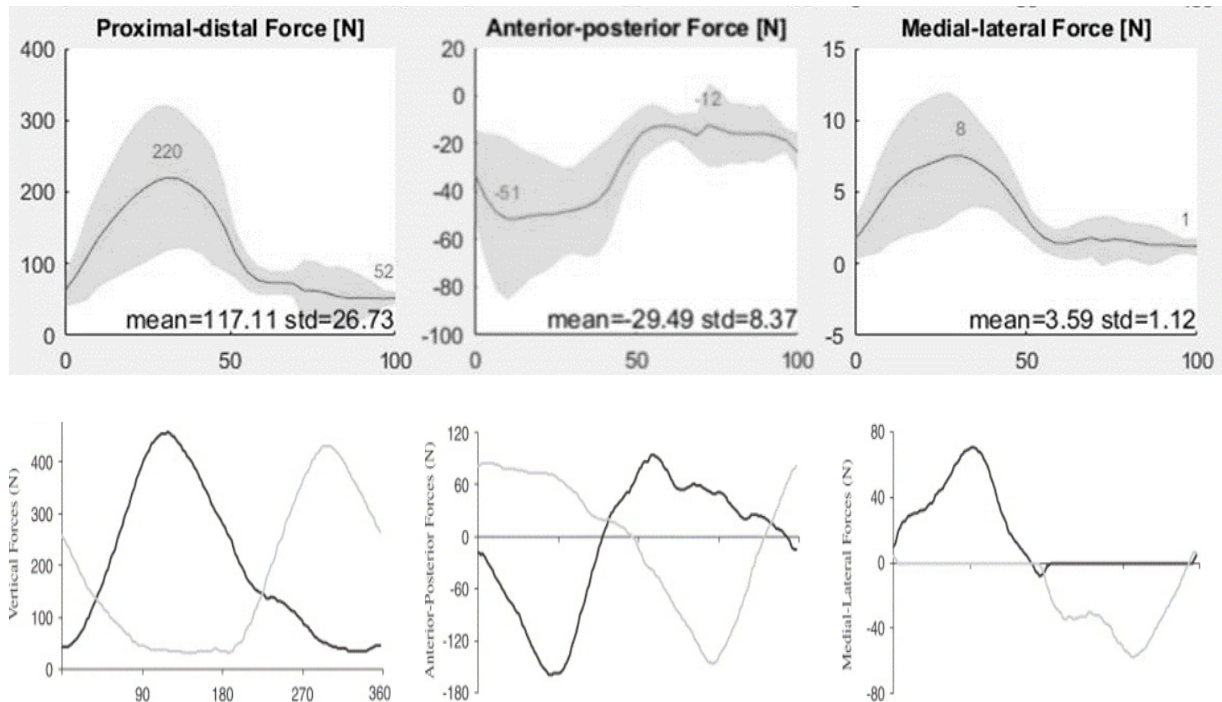


Fig. 6. Comparison of the cycling patterns of this research with those of Mornieux et al. (Mornieux, Zalezuatu, Mutter, Bonnefoy, & Belli, 2005)

5. CONCLUSION

The paper presents a low-cost strain gauge-based instrumented pedal differentiated from others like Mornieux, Dorel or Bini [12, 6, 21] with the following advantages: (i) it measures all three dimensional forces, not ignoring the medial-lateral ones that are accountable for severe knee injuries; (ii) it is designed in a way that producing accuracy has a marginal influence on the standard error (In this case, the standard error percentage of full scale reaches up to maximal 0.5%); (iii) the forces are related to crank arm which makes it possible to analyze standard pedal cycles and relate pedal patterns to overuse injuries and muscle fatigue; and (iv) the pedal does not compromise normal cycling; it is installable on conventional bicycles, the vertical distance between the pedal's lower surface and spindle is 17mm which prevents hitting the ground when turning and the vertical distance between the pedal's footplate and spindle is 17mm to adapt a normal pedal movement. Therefore, it is applicable for in-situ measurements as well as stationary ones.

Reference

1. Wannich, T. & Hodgkins, C. & Columbier, J.A. & Muraski, E. & Kennedy, J.G. Cycling injuries of the lower extremity. *Journal of the American Academy of Orthopaedic Surgeons*. Vol. 15(12). 2007. P. 748-756.
2. Dettori, N.J. & Norvel, D.C. Non-traumatic bicycle injuries: A review of the literature. *Sports Medicine*. Vol. 36(1). 2006. P. 7-18.
3. Hull, M.L. & Davis, R.R. Measurement of pedal loading in bicycling: I. Instrumentation. *Journal of biomechanics*. 1981. Vol. 14(12). P. 843-856.
4. Newmiller, J. & Hull, M.L. & Zajac, F.E. A mechanical decoupled two force component bicycle pedal dynamometer. *Journal of Biomechanics*. 1988. Vol. 21(5). P. 375-386.

5. Alvarez, G. & Vinyolas, J. A new bicycle pedal design for on-road measurements of cycling forces. *Journal of Applied Biomechanics*. 1996. Vol. 12(1). P. 130-142.
6. Dorel, S. & Drouet, J. & Hug, F. & Lepretre, P. & Champoux, Y. New instrumented pedals to quantify 2D forces at the shoe-pedal interface in ecological conditions: Preliminary study in elite cycling. *Computer Methods in Biomechanics and Biomechanical engineering*. 2008. Vol. 11. P. 89-90.
7. Hull, M.L & Gonzalez, H.K. The effect of pedal platform height on cycling biomechanics. *International Journal of Sports Mechanics*. 1990. No. 6. P. 1-17.
8. Millet, G.P. & Tronche, C. & Fuster, N. & Bentley D.J. & Candau, R. Validity and Reliability of the Polar S710 Mobile Cycling Powermeter. *International journal of sports medicine*. 2003. Vol. 24(3). P. 156-161.
9. Theurel, J. & Crepin, M. & Foissac, M. & Temprado, J.J. Effects of different pedalling techniques on muscle fatigue and mechanical efficiency during prolonged cycling. *Scandinavian Journal of Medicine & Science in Sports*. 2012. Vol. 22(6). P. 714-721.
10. Yanamashetti, G. & Murthy, H.S. Application of Global Regression method for Calibration of Wind Tunnel Sensors. In: *Symposium on Applied Aerodynamics and Design of Aerospace Vehicles*. 2011. Bangalore, India. 8 p.
11. Vanwalleghem, J. *Development of an experimental test platform for the static and dynamic evaluation of racing bicycle components and for measuring the dynamic bicycle-cycle interaction*. Gent: Universiteit Fent. 2015.
12. Mornieux, G. & Zalezuatu, K. & Mutter, E. & Bonnefoy, R. & Belli, A. A cycle ergometer mounted on a standard force platform for three-dimensional pedal forces measurement during cycling. *Journal of Biomechanics*. 2005. Vol. 39(3). P. 1293-1303.
13. Blandford, A. *Calibration for the Sensitivity Matrix of the Collins Strain Gauge Sensor*. Platforms Science Laboratory, Australia, 2004.
14. Nouri, N.M. & Mostafapour, K. & Kamran, M. & Bohadori, R. Design methodology of a six-component sensor for measuring forces in water tunnel tests. *Measurement*. 2014. No. 58. P. 544-555.
15. Lam, S.S. & Fairlie, B.D. A wind tunnel strain gauge sensor calibration system. In: *Twelfth Australian Fluid Mechanics Conference*. Australia, 1995. P. 155-158.
16. Boyd, T. & Hull, M.L. & Wootten, D. An improved accuracy six-load component pedal dynamometer for cycling. *Journal of Biomechanics*. 1996. Vol. 29(8). P. 1105-1110.
17. Broker, J.P. & Gregor, R.J. A dual piezoelectric element force pedal for kinetic analysis of cycling. *International Journal of Sport Biomechanics*. 1990. Vol. 6. No. 4. P. 394-403.
18. Ruby, P. & Hull, M.L. & Hawkins, D. Three-dimensional knee joint loading during seated cycling. *Journal of Biomechanics*. 1992. Vol. 25(1). P. 41-53.
19. Cannon, D.T. & Kolkhorst, F.W. & Cipriani, D.J. Effect of pedaling technique on muscle activity and cycling efficiency. *European Journal of Applied Physiology*. 2007. Vol. 99(6). P. 659-664.
20. Schwachmeyer, V. & Kutzner, I. & Bornschein, J. & Bender, A. & Dymke, J. & Bergmann, G. Medial and lateral foot loading and its effect on knee joint loading. *Clinical Biomechanics*. 2015. Vol. 30(8). P. 860-866.
21. Bini, R.R. & Diefenthaler, F. & Carpes, F.P. Determining force and power in cycling: A review of methods and instruments for pedal force and crank torque measurements. *International SportMed Journal*. 2014. Vol. 15(1). P. 96-112.